

# Correction for thermal distortions of laser beams with a flexible mirror. Experimental and numerical investigations

F Kanev<sup>1</sup>, N Makenova<sup>1</sup>, R Nesterov<sup>1</sup> and I Izmailov<sup>2</sup>

<sup>1</sup>Tomsk Polytechnic University, 30, Lenina ave., Tomsk, 634050, Russia

<sup>2</sup>Tomsk State University, 36, Lenina ave., Tomsk, 634050, Russia

E-mail: makenova@tpu.ru

**Abstract.** A mathematical model of an adaptive optics system was described in the article. The model included two main components: the model of an adaptive mirror and model of beam propagation under conditions of thermal blooming. Results of numerical simulation of adaptive optics systems were compared with data of laboratory experiments. High reliability of the model was shown.

## 1. Introduction

Adaptive optics systems are extensively used nowadays to correct distortions of laser beams propagating on atmospheric paths [1]. A schematic diagram of such system is shown in Figure 1. As is well known, beam propagating in the atmosphere suffers from random variations of the index of refraction and from thermal distortions induced by heating of the medium. As a result, in the plane of observations the amplitude profile of the beam is severely distorted. In adaptive systems the information about distortions transmitted by the loop to the active element which forms a phase profile of the beam according the algorithm of correction. Effectiveness of compensation for distortions depends on the precision of beam parameter registration, on the control algorithm of the system, on the rate of control, and on the quality of the phase profile formed by the active element. A flexible mirror with continuous reflecting surface is used usually as an active element of adaptive systems [2].

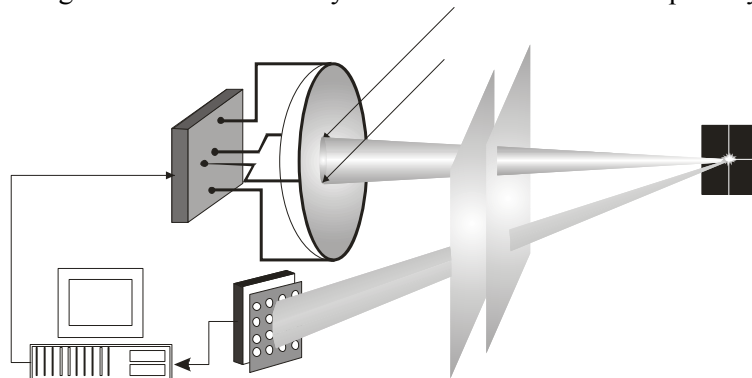


**Figure 1.** A schematic diagram of an adaptive optics system

In the current paper a model of the flexible mirror is presented along with a model of beam propagation in a medium. The results of numerical simulation are compared with the data of the



laboratory experiment, and the possibility of using a developed model in investigations of beam correction effectiveness is assessed.

## 2. A model of an adaptive optics system

The whole model of an adaptive system, as it follows from the diagram shown above (Figure 1), should include a model of a mirror, a model of beam propagation in a medium, and an algorithm of beam control. The model of the mirror used in our investigations was built on the basis of techniques developed by S. Chesnokov [3, 4]. The author assumed that an adaptive mirror can be represented as a thin plate controlled by forces applied at discrete points. After that the finite element method was applied to calculate deformations of the plate [4]. Application of the model in problems of adaptive optics was demonstrated in the numeric experiment simulating the multidither system of thermal blooming correction [5].

Following the papers by S. Chesnokov we extended the model. In the first publications on the subject we described the model with an increased number of actuators (from 4 to 20, Figure 2) and assessed its application in the phase conjugation algorithm [6, 7]. Along with the advanced technology of modern computers the limits on calculation grid dimensions were shifted, and control of the mirror surface was realised at 500 points. Also we developed a model of the adaptive corrector controlled by forces and by moments of forces which was used in simulation of the laboratory experiment of correction for thermal blooming [8].

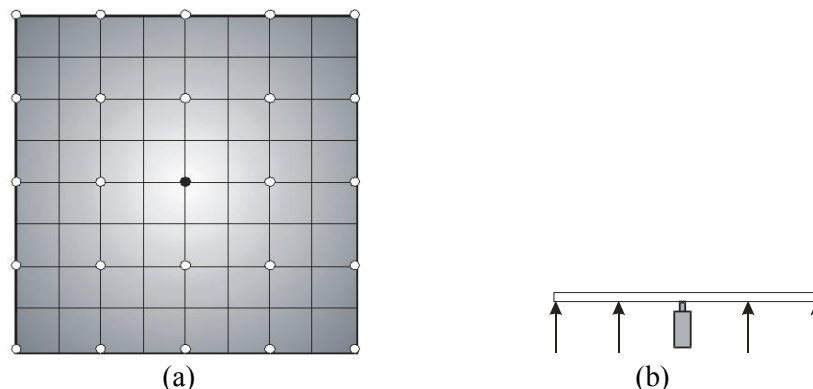


**Figure 2.** A model of the mirror controlled by forces applied at discrete points: a) top view, b) side view

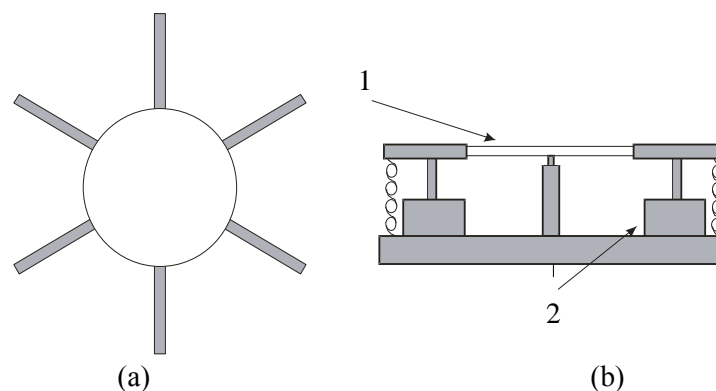


**Figure 3.** Model of the mirror controlled by moments of forces: a) top view; b) side view: 1-a stepper motor, 2 -a reflective surface

One more model developed for adaptive optics applications was a model of a dynamic mirror taking into account oscillations of the reflecting surface due to deformation of the plate [9]. In corresponding equations the mass and inertia of the plate were allowed for and transient processes were calculated [10]. Hence it follows that mathematical models of the listed above correctors are presented.

In approximation of a thin plate static deformations  $W(x,y)$  of the corrector can be described by the following equation [10]:

$$D \left( \frac{\partial^4 W}{\partial x^4} + 2 \frac{\partial^4 W}{\partial x^2 \partial y^2} + \frac{\partial^4 W}{\partial y^4} \right) = f(x, y). \quad (1)$$

Here  $x$  and  $y$  are Cartesian coordinates in the plane of the mirror,  $D = Eh^3 / (12(1 - \sigma^2))$  is cylindrical rigidity,  $\sigma$  is the Poisson coefficient,  $E$  is Young's modulus,  $h$  is thickness of the plate, and  $f(x, y)$  are a load applied normally to the plate.

If the plate is controlled by a system of discrete forces  $P_j$ , the load can be represented in the form:

$$f(x, y) = \sum_{j=1}^v P_j \delta(x - x_j, y - y_j) S_j, \quad (2)$$

$x_j$  and  $y_j$  – are coordinates of actuators,  $S_j$  is its area, and  $v$  is the number of actuators.

Border conditions should be written for all points of plate contour  $L$ . Conditions characterizing free edges of the plate can be formulated as:

$$D \left( \frac{\partial^2 W}{\partial n^2} + \sigma \frac{\partial^2 W}{\partial \tau^2} \right) \Big|_{L_j} = 0, \quad D \frac{\partial}{\partial n} \left( \frac{\partial^2 W}{\partial n^2} + (2 - \sigma) \frac{\partial^2 W}{\partial \tau^2} \right) \Big|_{L_j} = 0.$$

Here  $\partial/\partial n$  and  $\partial/\partial \tau$  are normal and tangential partial derivatives correspondingly.

If normal force  $P_j$  and moment  $T_j$  are applied to points  $L_j$  on the perimeter of the plate, the border conditions should be changed to the form:

$$D \left( \frac{\partial^2 W}{\partial n^2} + \sigma \frac{\partial^2 W}{\partial \tau^2} \right) \Big|_{L_j} = \frac{-T_j \delta(x - x_j, y - y_j)}{l_j},$$

$$D \frac{\partial}{\partial n} \left( \frac{\partial^2 W}{\partial n^2} + (2 - \sigma) \frac{\partial^2 W}{\partial \tau^2} \right) \Big|_{L_j} = \frac{-P_j \delta(x - x_j, y - y_j)}{l_j},$$

where  $x_j$  and  $y_j$  are coordinates of the point where the force is applied, and  $l_j$  is a distance between points.

Conditions corresponding to the points inside the contour of the plate can be written in the same way, for example, if a point fixed rigidly:

$$W(0,0) = \frac{\partial W(0,0)}{\partial x} = \frac{\partial W(0,0)}{\partial y} = 0.$$

Solution to Eq. 1 with the border conditions given above is difficult to obtain analytically, so numerical models of the mirror were developed on the basis of the finite element method [4]. According to the method, all surface of plate  $W(x,y)$  is divided into small sections  $\Omega$  (finite elements), and in each section a local coordinate system with axes  $O\xi, O\eta$  is set up. So instead of calculation of the whole plate deformation, we determine only deformation of each finite element  $W(\xi, \eta)$ . Elements should be joined by cinematic and dynamic border conditions, so the total set of finite elements forms the model of the whole plate.

Consecutively, the shape of finite element surface  $W(\xi, \eta)$  is approximated by a linear form of base functions  $\mathbf{III}(\xi, \eta)$ :

$$W(\xi, \eta) = \mathbf{III}^T(\xi, \eta) \mathbf{a} \mathbf{q}. \quad (3)$$

Here  $\mathbf{III}^T(\xi, \eta)$  is a vector of base functions, and superscript 'T' signifies the operation of a vector transposing.  $\mathbf{a}$  is a matrix of coordinates transformation and  $\mathbf{q}$  is a vector of generalized coordinates. As generalized coordinates shifts  $W_r$  and tilts  $\varphi_r, \nu_r$  in nodes of the calculation grid are taken usually as [3, 4], so in each node (the number of nodes is  $R$ ) the model is characterized by three variables.

The vector of generalized nodal forces

$$\mathbf{Q} = \begin{pmatrix} \mathbf{P} \\ \mathbf{N} \\ \mathbf{T} \end{pmatrix} \quad (4)$$

is conjugated with coordinate vector  $\mathbf{q}$ . In Eq. 4  $\mathbf{P}$  is a vector of normal forces and vectors  $\mathbf{N}$  and  $\mathbf{T}$  are vector of force moments relatively axes  $o\xi$  and  $o\eta$ .

The principle of virtual displacements is possible to apply in order to obtain equation relating vectors  $\mathbf{q}$  and  $\mathbf{Q}$  [3]:

$$-\delta U + \delta A_m + \delta A_f + \delta A_Q = 0. \quad (5)$$

In Eq. 5  $\delta U$  is variation of the element potential energy,  $\delta A_m$  is the virtual work of inertia forces,  $\delta A_f$  is virtual work of applied load, and  $\delta A_Q = \delta \mathbf{q}^T \mathbf{Q}$  is the work of forces of interactions.

To obtain the equation describing deformation of the whole model we should, firstly, take into account continuity of the generalized coordinates in the nodes of the calculation grid and, secondly, equilibrium of forces in these nodes. As a result,

$$\|\mathbf{M}\| \ddot{\mathbf{W}}(x, y) + \|\mathbf{G}\| \dot{\mathbf{W}}(x, y) + \|\mathbf{K}\| \mathbf{W}(x, y) = \mathbf{Q}_f. \quad (6)$$

Matrices  $\|\mathbf{M}\|$ ,  $\|\mathbf{G}\|$ , and  $\|\mathbf{K}\|$  have the same meaning as those described earlier, but now they are written for the whole model.  $\|\mathbf{Q}_f\|$  is a vector of external forces applied to the plate. A solution to Eq. 6 is possible to find with application of numeric methods, and in this particular problem Runge-Kutta method was used [11].

Calculation of static deformations allows one to simplify Eq. 6 and obtain the formula:

$$\|\mathbf{K}\| \mathbf{W}(x, y) = \mathbf{Q}_f, \quad (7)$$

so the shape of the plate can be found as

$$\mathbf{W}(x, y) = \|\mathbf{L}\| \mathbf{Q}_f, \quad (8)$$

here  $\|\mathbf{L}\| = \|\mathbf{K}\|^{-1}$  is a matrix inverse relatively to  $\|\mathbf{K}\|$ .

Another model required in numerical experiments is a model of beam propagation in an atmosphere. Propagation of a beam in the randomly inhomogeneous absorbing medium is characterized by the wave equation written in the approximation of quasioptics:

$$2ik \frac{\partial E}{\partial z} = \frac{\partial^2 E}{\partial x^2} + \frac{\partial^2 E}{\partial y^2} + \frac{k^2}{n_0} \tilde{n} + n_{nl} E, \quad (9)$$

where  $E = E(x, y, z, t)$  is the complex amplitude of the field,  $k = 2\pi/\lambda$  is a wave number,  $\lambda$  is a wave length. Variables in the problem were normalized as follows: in the direction of the laser beam propagation ( $Z$ -axis) on the diffraction length  $Z_d = ka_0^2$  ( $Z = Z/Z_d$ ), and in the direction perpendicular to the path on the initial radius of the beam  $a_0$  ( $x = x/a_0, y = y/a_0$ ). In Eq. 9  $\tilde{n}$  is random fluctuations of the refractive index induced by turbulence (not taken into account), and  $n_{nl}$  is variations induced by heating of the medium. The influence of heating on the laser beam form is called the effect of thermal blooming. Eq. 8 was solved with the use of the splitting method.

### 3. Comparison of experimental results with results of numerical simulation

To validate the developed model of an adaptive system the results of numerical experiments were compared with the data found in references. Particularly, variables characterizing the model were put in correspondence to parameters of the mirror built at the Institute of Optics and Electronics, Chinese Academy of Sciences [12]. The parameters of the mirror were the following: the diameter was 20 mm; the maximum shift of the reflecting surface –  $\pm 1.0 \mu\text{m}$ , and the resonance frequency – 30 kHz. The mirror was controlled by 19 actuators attached to the plate at discrete points. Calculation of actuator response functions demonstrated a 10% deviation of numerical results from the published characteristic of the mirror. High precision of the model was assumed.

One more opportunity to compare theoretical and experimental data emerged after publication of the experimental results of correction for thermal blooming [13]. In the optical system employed in the investigations the phase profile of radiation was formed by the flexible mirror controlled by moments of forces. Schematically the mirror is shown in Figure 3. Distortions of the beam were developed as a result of propagation in a cell filled by semitransparent liquid. The flux of the medium was simulated by rotation of the cell. The amplitude distribution of the beam was registered by a video camera, and the main characteristics of the radiation, such as shifts  $x_C$  and  $y_C$  of the beam centroid in Cartesian coordinate system, radii  $\sigma_x$  and  $\sigma_y$ , as well as maximum intensity  $I_m$  are calculated by a specially developed software. The information obtained as a result of calculations was used for generation of mirror control signals. Adaptive correction was realized with the use of the multidither algorithm. The vector characterizing amplitude distribution of the beam was chosen as a goal function of correction. Vector  $\mathbf{J}$  had the following components:

$$J_1 = x_0 - x_C; J_2 = y_0 - y_C; J_3 = \sigma^2 - \sigma_0^2;$$

$$J_4 = \sigma_x^2 - \sigma_y^2; J_5 = \sigma_{xx}; J_6 = \sigma_x^2 + \sigma_y^2.$$

Here  $\sigma_0$  is the radius fan undistorted beam.

A qualitative comparison of results was made with the use of photographs of laser beam amplitude profiles taken before and after correction (Figure 4).

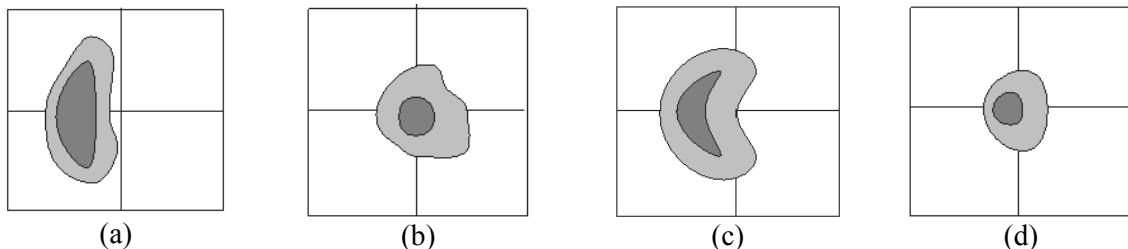


**Figure 4.** Comparison of experimental and theoretical results. The beam amplitude profile registered experimentally before (a) and after correction (b). Corresponding results obtained in numerical experiment (c and d)

In the same picture the profiles registered in numerical experiments were presented. As one can see, the beam shape and its changes are practically the same in both cases.

A comparison of results in absolute units was impossible so we introduced a relative criterion characterizing the effectiveness of correction:

$$\eta_J = \left( \frac{J_{opt} - J_0}{J_0} \right) \cdot 100\% ,$$

here  $J_{opt}$  is some parameter of the beam (radius, maximum intensity, or centroid shift) obtained as result of correction and  $J_0$  is the same parameter registered before application of adaptive control. Experimentally obtained criteria  $\eta_{\sigma_x}$ ,  $\eta_{\sigma_y}$ ,  $\eta_{I_m}$  describing changes of radii  $\sigma_x$ ,  $\sigma_y$  and maximum intensity of the beam  $I_m$  are presented in Table 1. In the same table the results of numerical simulation are shown.

**Table 1.** Experimental and theoretical results

	$\eta_{\sigma_x}$	$\eta_{\sigma_y}$	$\eta_{I_m}$
Laboratory experiment	-24	-55	107
Numerical experiment	-26	-50	344

As one can see the largest discrepancy was registered for maximum intensity of the beam  $I_m$ , but this variable is a local characteristic of the beam measured with less precision as compared to its integral characteristics  $\sigma_x$  and  $\sigma_y$ .

#### 4. Conclusions

The experimental data and results of numerical investigations presented here have demonstrated high reliability of the developed model. The model can be used in simulation of real experiments in adaptive optics.

#### References

- [1] Tyson R 1991 *San Diego: Academic Press* 233
- [2] Cherezova T *et al* 1999 *Proc. of the 2-rd International Workshop on Adaptive Optics for Industry and Medicine* 187-192
- [3] Vorontsov M and Chesnokov S 1982 *Radiophysics* vol **25** 11
- [4] Kandidov V, Chesnokov S and Vislouxh V 1976 *Moscow State University Publ. House* 178
- [5] Chesnokov S 1983 *Quantum electronics* **10** 6
- [6] Kanev F, Lukin V and Lavrinova L 1994 *Atmospheric propagation and remote sensing III Orlando, USA* 57-58
- [7] Kanev F, Lukin V and Fortes B 1995 *Internet Geoscience and Remote Sensing Symposium Firenze, Italy* 5
- [8] Kanev F and Lukin V 1991 *Atmospheric optics* **4** 12
- [9] Kanev F 1990 *Conference Lasers and atmosphere (Obninsk)* 161
- [10] Ogibalov P 1958 *Moscow State University Publishing House* 168
- [11] Potter D 1975 *Moscow: Mir publishers* 376
- [12] Ling N and Guan Ch 1996 *SPIE Proc.* **2828** 472-478
- [13] Kandidov V, Larionova I and Popov V 1989 *Atmospheric optics* **2** 8